Journal of Nuclear Materials 378 (2008) 55–59

Contents lists available at ScienceDirect

Journal of Nuclear Materials

journal homepage: www.elsevier.com/locate/jnucmat

On the effects of fission product noble metal inclusions on the kinetics of radiation induced dissolution of spent nuclear fuel

Martin Trummer, Sara Nilsson, Mats Jonsson *

KTH Chemical Science and Engineering, Nuclear Chemistry, Royal Institute of Technology, SE – 100 44 Stockholm, Sweden

ARTICLE INFO

Article history:
Received 14 January 2008
Accepted 24 April 2008

ABSTRACT

Radiation induced oxidative dissolution of UO_2 is a key process for the safety assessment of future geological repositories for spent nuclear fuel. This process is expected to govern the rate of radionuclide release to the biosphere. In this work, we have studied the catalytic effects of fission product noble metal inclusions on the kinetics of radiation induced dissolution of spent nuclear fuel. The experimental studies were performed using UO_2 pellets containing 0%, 0.1%, 1% and 3% Pd as a model for spent nuclear fuel. H_2O_2 was used as a model for radiolytical oxidants (previous studies have shown that H_2O_2 is the most important oxidant in such systems). The pellets were immersed in aqueous solution containing H_2O_2 and HCO_3^- and the consumption of H_2O_2 and the dissolution of uranium were analyzed as a function of H_2 pressure (0–40 bar). The noble metal inclusions were found to catalyze oxidation of UO_2 as well as reduction of surface bound oxidized UO_2 by H_2. In both cases the rate of the process increases with increasing Pd content. The reduction process was found to be close to diffusion controlled. This process can fully account for the inhibiting effect of H_2 observed in several studies on spent nuclear fuel dissolution.

1. Introduction

Radioactive waste is one of the major drawbacks of nuclear power today where the long-lived radionuclides in spent nuclear fuel constitute the largest problem. In several countries, there are highly developed plans to place the spent nuclear fuel in geological repositories where a multiple barrier system will protect the spent nuclear fuel from groundwater and prevent radionuclides from escaping the repository in the event of groundwater intrusion. The safety of such a repository relies on the long term efficiency of the barriers. In general, for UO_2 based fuel, the innermost barrier protecting the fission products and heavier actinides from escaping the repository is the fuel matrix itself. After use in the nuclear reactor, the spent nuclear fuel still contains more than 95% UO_2. UO_2 has very low solubility under the reducing conditions prevailing in a potential deep repository in granitic bedrock (e.g., in Sweden) and could thus be considered to be an efficient barrier [1–3]. However, the inherent radioactivity of the spent nuclear fuel will induce radiolysis of groundwater in contact with the fuel. Radiolysis of water produces equal amounts of oxidants and reductants [4]. For kinetic reasons, the oxidants will have the largest impact on the local environment [5]. The net effect will be oxidation of U(IV) to the significantly more soluble U(VI). Hence, radiolysis will induce oxidative dissolution of the fuel matrix. The general mechanism for this process is given.

$$UO_2(S) + OX \rightarrow UO_2^{2+}(S) + RED, \quad (1)$$

$$UO_2^{2+}(S) \rightarrow UO_2^{2+}(aq). \quad (2)$$

The dissolution of oxidized UO_2 has been found to be enhanced by the presence of HCO_3^- which forms strong, water soluble, complexes with UO_2^{2+} [6–10].

Dissolution of UO_2 and spent nuclear fuel has been extensively studied [5,11 and references therein]. Indeed, the system is very complex and it can be difficult to draw any mechanistic conclusions from experiments using spent nuclear fuel. One way of circumventing this problem has been to study the elementary processes involved using simple model systems, such as pure UO_2 [12]. In this way, the rate constants for oxidation of UO_2 by a number of oxidants have been determined along with the rate constants for HCO_3^- facilitated dissolution of oxidized UO_2 and dissolution of oxidized UO_2 in pure water [13]. Using kinetic data and numerical simulations of radiolysis in aqueous solution the relative impact of the different radiolytical oxidants has been determined [14]. This determination was also verified by well controlled experiments on radiation induced oxidative dissolution of UO_2. These studies show that H_2O_2 is by far the most important oxidant in spent nuclear fuel under deep repository conditions. Hence, if the surface concentration of H_2O_2 can be calculated, the rate of UO_2 oxidation can also be calculated. The rate of H_2O_2 production is proportional to the dose rate [15].

Models describing the geometrical dose distribution (dose rate as a function of distance from fuel surface) on the basis of the radionuclide inventory have also been developed in recent years [16].

* Corresponding author. Tel.: +46 8 790 9123; fax: +46 8 790 8772.
E-mail address: matsj@kth.se (M. Jonsson).

0022-3115/$ - see front matter © 2008 Elsevier B.V. All rights reserved.
doi:10.1016/j.jnucmat.2008.04.018

Simulations of the evolution of the H_2O_2 concentration profile taking into account the geometrical dose distribution, the reaction between H_2O_2 and the UO_2 surface and diffusion of H_2O_2 show that the H_2O_2 surface concentration approaches a constant value fairly rapidly [15]. This constant value corresponds to the system steady-state concentration. Consequently, the rate of UO_2 oxidation is constant and can be directly calculated from the dose rate. This simplifies simulation of spent nuclear fuel dissolution dramatically. The steady-state approach has been used to predict dissolution rates for systems where experimental results are also available [17,18]. The agreement between the predicted rate and the experimental data is surprisingly good.

In recent years, considerable efforts to elucidate the effect of H_2 on the dissolution of spent nuclear fuel have been made [19–21]. H_2 is produced by radiolysis of water and also by anaerobic corrosion of iron in the canister for spent fuel. The latter process is expected to produce considerable amounts of H_2. Spent nuclear fuel leaching experiments performed under H_2 atmosphere display a different behaviour from analogous experiments performed under anoxic conditions in the absence of H_2. In the presence of H_2 the rate of fuel matrix (UO_2) dissolution is greatly reduced and in some cases completely inhibited [21]. Furthermore, long term leaching experiments performed in sealed vessels, initially under Argon atmosphere, show that the rate of dissolution decreases with time (and increasing H_2 concentration produced upon radiolysis of water) [22]. The rationale for this has not been clarified and several theories aiming at explaining the inhibiting effect of H_2 have been put forward. Electrochemical experiments have shown that the corrosion potential of synthetic spent nuclear fuel (SIMFUEL) containing noble metal inclusions mimicking clusters of fission products (the clusters normally contain Mo, Ru, Tc, Rh, Pd and Te and are often referred to as ε-particles) is greatly reduced under H_2 atmosphere compared to anoxic conditions without H_2 [23]. The corrosion potential (which is related to the rate of oxidative dissolution) was found to depend on the H_2 partial pressure over the total pressure range 0–0.21 MPa. In the absence of ε-particles no substantial change in corrosion potential can be observed in solutions saturated with a H_2 containing gas mixture or pure Ar. The proposed explanation is a catalytic H_2-dissociation reaction on these particles which act as galvanic anodes within the fuel matrix and causes reduction of oxidized uranium. The net effect would be recombination of H_2O_2 and H_2 to H_2O.

Recent kinetic studies have shown that the recombination of H_2O_2 and H_2 on noble metal (Pd) particles is a virtually diffusion controlled process [24]. The potential catalytic decomposition of H_2O_2 on Pd was shown to be considerably slower (insignificant compared to the reaction between H_2O_2 and H_2 on Pd). However, considering the amount of fission products present in spent nuclear fuel, the Pd catalyzed reaction alone would not be able to compete efficiently with the reaction between H_2O_2 and UO_2. Even though the rate constant for the reaction between H_2O_2 and UO_2 is approximately 20 times lower than the rate constant for the Pd (noble metal) catalyzed reaction between H_2O_2 and H_2, the ratio between UO_2 and noble metal particles is around 100. This means that the majority of the H_2O_2 will be consumed in the reaction with UO_2 and the rate of oxidation will only be slightly reduced. Under steady-state conditions (where the rate of radiolytical production of H_2O_2 is equal to the rate of H_2O_2 consumption via surface reactions) the effect will be slightly larger. Consequently, the mere catalysis of the reaction between H_2O_2 and H_2 is not a sufficient explanation for the observed effect. It should also be noted that it has been shown experimentally that UO_2 does not catalyze the reaction between H_2O_2 and H_2 [24]. Pd-particles have also been shown to catalyze the reduction of UO_2^{2+}(aq) by H_2 efficiently (diffusion controlled kinetics) [25]. This process could indeed account for reduced concentrations of uranium in solution. It should be noted that experiments displaying inhibition of uranium dissolution also display general inhibition of fission product and actinide dissolution [18,20,21]. Hence, reduction of already dissolved uranium catalyzed by noble metal particles does not provide an explanation for the observed phenomenon. Had this been the case, the dissolution of redox insensitive elements such as Cs^+ and Sr^{2+} would not have been affected by the presence of H_2.

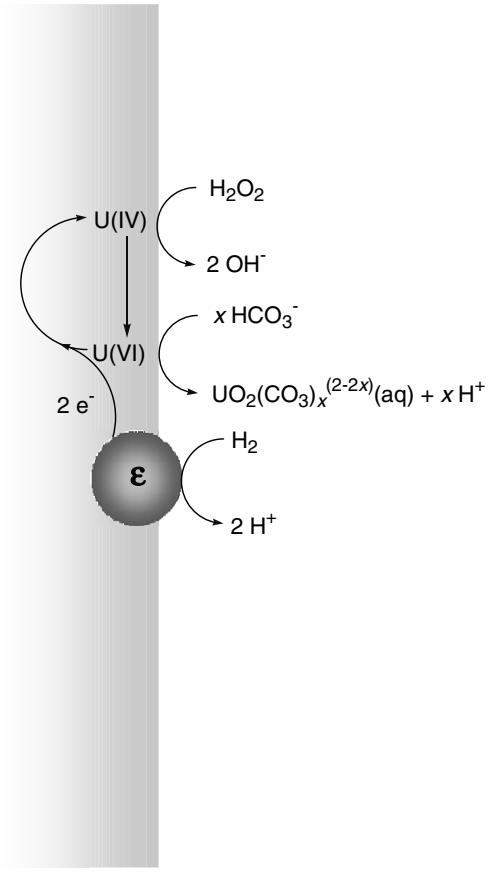

Scheme 1. Processes causing oxidative dissolution of UO_2 and noble metal particle catalyzed H_2-inhibition.

The simplest and most straight forward explanation to the experimental observations is a noble metal catalyzed solid phase or surface reduction of U(VI) by H_2 as suggested by Broczkowski et al. [23] and discussed in [24,25]. This process and the processes causing oxidative dissolution of UO_2 are illustrated in Scheme 1.

The solid phase or surface reduction of UO_2^{2+} by H_2 competes with HCO_3^- facilitated dissolution of UO_2^{2+} and when the rate of reduction is equal or higher than the rate of dissolution, full inhibition can be observed. On the basis of kinetic constraints, this process has the potential to completely inhibit UO_2 dissolution under deep repository conditions.

In the present paper, we have studied the impact of the proposed solid phase or surface reduction by analysing the influence of H_2 on the dissolution of uranium from UO_2 pellets doped with Pd-particles using H_2O_2 as oxidant in HCO_3^- containing solutions.

2. Experimental

The depleted uranium dioxide powder came from Westinghouse Atom AB. The sodium hydrogen carbonate solution was prepared with $NaHCO_3$ p.a. from Merck and the water used throughout the experiments was Millipore Milli-Q. The potassium iodide powder puriss came from KEBO Lab. The palladium powder

with a purity of 99.9+% had an average particle size of 1.0–1.5 μm and was manufactured by Aldrich. The Arsenazo III reagent was prepared from p.a. powder from Fluka.

UO_2 pellets doped with Pd-particles were manufactured by hot-pressing using equipment from Thermal Technology INC (model 1000A). The form for pressing the pellets was made of graphite covered with boron nitride as a lubricant. Four different pellets were produced. One pellet containing only UO_2 and three pellets containing different amounts of palladium.

Prior to the pressing, the powder was washed three times with 10 mM hydrogen carbonate solution to remove U(VI) and then filtrated by vacuum filtration. The powder was then dried for 48 h under vacuum, and mixed with palladium powder when applicable. The whole mixture was then stored under argon atmosphere until it got pressed.

A temperature of 1200 °C and a pressure of 40 MPa was used in order to hot-press the pellets. The powder was first cold-pressed at a pressure of 20 MPa to pre-compact it and then the pressure and the temperature were increased simultaneously to their final values, the latter at a heating rate of around 40 °C/min, so that the final temperature was reached after 30 min. The form used had a diameter of 13 mm and the pellets a thickness of 2.6 mm, leading to a surface area of 371.7 mm^2. During the whole process vacuum was applied.

After 1 h, the pressure was removed, the induction heater was turned off and the form was taken out after 4 h, shortly after it had reached room temperature. The one-time inner form was crushed in order to get out the sample without producing unnecessary stress in the pellet.

The pellet was covered by a thin layer of boron nitride after pressing, which had to be removed by wet grinding with silicon carbide abrasive paper. A paper with fine silicon carbide particles was chosen in order not to do damage to the surface of the pellet. Furthermore it was necessary to wash the pellet in 10 mM HCO_3^- solution after grinding and also before every experiment in order to remove oxidized UO_2 from the surface.

The oxidative dissolution experiments were performed in 10 mL aqueous solutions containing 10 mM HCO_3^- and H_2O_2. The solutions were saturated with N_2 or H_2. When using H_2, various pressures were applied during the dissolution experiments. The concentrations of H_2O_2 and U(VI) were measured when the experiment was initiated and after 50 min. All experiments were performed at room temperature using glass vessels placed in a stainless steel autoclave. The concentration of H_2O_2 was measured by UV–vis spectroscopy using I_3^- as a monitor.

$$2I^- + H_2O_2 \rightarrow I_2 + 2OH^-, \quad (3)$$

$$I_2 + I^- \rightarrow I_3^-. \quad (4)$$

The sample was diluted by a factor of 100 with water, and 300 μL of that solution was mixed with 100 μL 1 M KI, 100 μL 1 M $NaOOCCH_3$/1 M HOAc and 1.5 mL H_2O and then measured at a wavelength of 360 nm. The uranyl concentration was also measured by UV–vis spectroscopy at 653 nm with the Arsenazo III method [26,27]. 950 μL of sample, 400 μL 0.03% arsenazo III reagent (3,6-bis[(2-arsonophenyl)-azo]-4,5-dihydroxy-2,7-naphtalenedisulphonic acid) and 650 μL 1 M HCl were mixed for that purpose.

3. Results and discussion

The solid surface area to solution volume ratio used in the experiments is fairly low. For this reason the consumption of H_2O_2 does not follow first order kinetics. Instead, the experiments were designed so that only a minor fraction of the H_2O_2 was consumed, i.e., the rate of oxidation is expected to be essentially constant during the experiment. However, initially the rate of oxidation will be slightly higher than the rate of dissolution until a steady-state is reached. At steady-state, the rate of UO_2 oxidation is equal to the rate of UO_2^{2+} dissolution.

$$k_{ox}[H_2O_2]SA(UO_2) = k_{HCO_3^-}[HCO_3^-]SA(UO_2^{2+}), \quad (5)$$

where $SA(UO_2)$ is the surface area of UO_2, k_{ox} is the rate constant for oxidation of UO_2 by H_2O_2 (7.3×10^{-8} m s^{-1}) [13], $k_{HCO_3^-}$ is the rate constant for HCO_3^- facilitated dissolution of UO_2^{2+} (1×10^{-6} m s^{-1}) [13] and $SA(UO_2^{2+})$ is the surface area of oxidized UO_2 (i.e., UO_2^{2+}). The total surface area is the sum of these surface areas. Given the fact that k_{ox} is lower than $k_{HCO_3^-}$ and $[H_2O_2]$ is lower than $[HCO_3^-]$ the surface area of oxidized UO_2 ($SA(UO_2^{2+})$) will be considerably lower than the UO_2 surface area ($SA(UO_2)$) at steady-state. The ratio of oxidized to non-oxidized surface area will be 0.15–1.5% in the experiments performed in this work. The volume used in the experiments was chosen so that detectable concentration of uranium in solution could be obtained at the same time as significant reduction in H_2O_2 concentration could be expected. In Table 1 data for a set of experiments using aqueous solution containing $[H_2O_2] = 0.2$ mM and saturated with N_2 or pressurized with H_2 (40 bar) are presented.

From the experiments performed under N_2 atmosphere it is obvious that the consumption of H_2O_2 and the dissolution of U(VI) is not balanced. However, it should be kept in mind that the system is not at steady-state from the beginning. Initially, the rate of consumption of H_2O_2 will be significantly higher than the rate of U(VI) dissolution. For this reason the change in concentrations will never match each other even after steady-state is reached. For the experiments performed under N_2 atmosphere it is also interesting to note that the consumption of H_2O_2 is virtually the same for all pellets while the amount of dissolved U(VI) appears to increase with increasing concentration of Pd in the pellet.

The experiments performed under H_2 pressure clearly show that the amount of dissolved U(VI) decreases with increasing Pd concentration while the amount of consumed H_2O_2 increases with increasing Pd concentration. However, the trends are not completely clear and for this reason we also performed experiments at 2 mM H_2O_2 (as this would give higher concentrations of U(VI) in solution). The results from this study are presented in Table 2.

As can be seen when comparing Tables 1 and 2, the consumption of H_2O_2 under N_2 atmosphere increases by one order of magnitude when increasing the H_2O_2 concentration by a factor of 10. The amount of dissolved U(VI) is also increased but by less than one order of magnitude. Under these conditions it becomes clear that dissolution of U(VI) in the absence of H_2 increases with increasing Pd concentration. This trend is demonstrated in Fig. 1.

As can be seen, the correlation between the amount of dissolved U(VI) and the Pd loading in the UO_2 pellets appears to be almost linear. The rationale for this is most probably that Pd catalyzes the oxidation of UO_2 by H_2O_2. The increase in amount of dissolved U(VI) is about a factor of five when increasing the Pd loading from 0% to 3%. This corresponds to a five fold increase in $SA(UO_2^{2+})$ at steady-state. From Eq. (5) it is obvious that an increase in k_{ox} will

Table 1
Uranyl dissolution and hydrogen peroxide consumption after 50 min ($[H_2O_2]_0 = 0.2$ mM)

Pd content (%)	UO_2^{2+} dissolution/μmol dm^{-3}		H_2O_2 consumption/mmol dm^{-3}	
	N_2	H_2	N_2	H_2
0	2.8	4.1	0.020	0.032
0.1	4.2	1.9	0.017	0.030
1	9.7	0	0.022	0.048
3	8.0	0	0.019	0.066

10% experimental uncertainty.

Table 2
Uranyl dissolution and hydrogen peroxide consumption after 50 min ($[H_2O_2]_0$ = 2.0 mM)

Pd content (%)	N_2	H_2 0.15 bar	H_2 1 bar	H_2 2 bar	H_2 20 bar	H_2 40 bar
	UO_2^{2+} dissolution/μmol dm^{-3}					
0	8.0	3.7	4.9	3.1	3.2	3.2
0.1	6.9	5.0	6.4	5.7	5.6	4.2
1	15	14	3.4	2.8	1.1	0.6
3	35	39	4.3	0.6	0.7	0.04
	H_2O_2 consumption/mmol dm^{-3}					
0	0.15	0.19	0.11	0.15	0.16	0.08
0.1	0.16	0.18	0.08	0.20	0.20	0.22
1	0.25	0.26	0.29	0.37	0.49	0.52
3	0.31	0.22	0.26	0.46	0.54	0.56

10% experimental uncertainty.

result in a shift in the UO_2^{2+}/UO_2 surface area ratio towards higher values. The surface area of available UO_2 will decrease. This will to some extent counteract the increase in rate constant. In fact, an increase in H_2O_2 consumption can be observed with increasing Pd loading at the higher initial H_2O_2 concentration under N_2 atmosphere (see Table 2).

The experiments performed at various partial pressures of H_2 clearly reveal that, for the pellets containing 1% and 3% Pd, the amount of dissolved U(VI) decreases with increasing H_2 pressure. It is also obvious that the magnitude of the reduction in amount of dissolved U(VI) increases with increasing Pd concentration. The H_2O_2 consumption also increases with increasing H_2 pressure for the Pd containing pellets. The magnitude of this relative change is, however, much smaller than for the dissolution of U(VI). Indeed, the processes described above (Pd catalyzed reaction between H_2O_2 and H_2 and Pd catalyzed reaction between H_2 and UO_2^{2+}(aq)) could account for some of these changes. The Pd catalyzed reaction between H_2O_2 and H_2 would, however, only reduce the rate of oxidation marginally as this rate depends on the H_2O_2 concentration and the accessible UO_2 surface area [24]. It should be stressed that while the H_2O_2 consumption increases by a factor of two (3% Pd) when going from N_2 to 40 bar H_2, the U(VI) dissolution is reduced by almost three orders of magnitude. The rate of oxidation is given by $r_{ox} = k_{ox}[H_2O_2]SA(UO_2)$ regardless of competing reactions. Competing reactions (e.g., Pd catalyzed reaction between H_2 and H_2O_2) will only influence the H_2O_2 concentration. For the pellet containing 3% Pd the final H_2O_2 concentration is 1.7 mM when using N_2 and 1.4 mM at 40 bar H_2. Consequently, the rate of oxidation cannot be more than 20% higher in the first case and competing reactions consuming H_2O_2 cannot explain the dramatic reduction in U(VI) dissolution. The increasing H_2O_2 consumption with increasing H_2 pressure for the pellets containing 1% and 3% Pd can be quantitatively attributed to the Pd catalyzed reaction between H_2O_2 and H_2. Taking the solid phase or surface reduction into account, the rate of oxidative UO_2 dissolution can be described by Eq. (6) [17].

$$r_{diss} = r_{ox} - k_{H_2}[H_2]\varepsilon_{rel}, \quad (6)$$

where r_{diss} is the dissolution rate, r_{ox} is the oxidation rate (i.e., the rate of oxidant consumption), k_{H_2} is the rate constant for the reaction between H_2 and the ε-particles, $[H_2]$ is the concentration of H_2 and ε_{rel} is the fraction of the fuel surface area covered by ε-particles. In Fig. 2, the ratio of the uranium dissolution rate in the presence of various concentrations of H_2 (r_{diss}) compared to the dissolution rate in the absence of H_2 ($r_{diss} = r_{ox}$) is plotted against the fraction of the surface area covered by Pd-particles (%) multiplied by the H_2 pressure.

As can be seen the rate of dissolution drops rapidly with increasing surface fraction of Pd (from 0% to 1% and 3%) in combination with increasing H_2 pressure. It is interesting to note that the inhibiting effect of H_2 remains even when the pellet is no longer exposed to H_2. Performing several consecutive experiments without H_2 after initial exposure to H_2 shows that the effect gradually decreases and that vacuum treatment enhances the recovery of the pellet. This behaviour is illustrated in Fig. 3.

Judging from Fig. 2 the oxidative dissolution process appears to become completely inhibited. Interestingly, the pellet containing 1% Pd appears to require a higher value of $\varepsilon \times pH_2$ for complete inhibition than the pellet containing 3% Pd. Using Eq. (6) we can estimate the rate constant for the solid phase or surface reduction process from the value of $\varepsilon \times pH_2$ where dissolution is cancelled. At this point the rate constant can be calculated from the following expression:

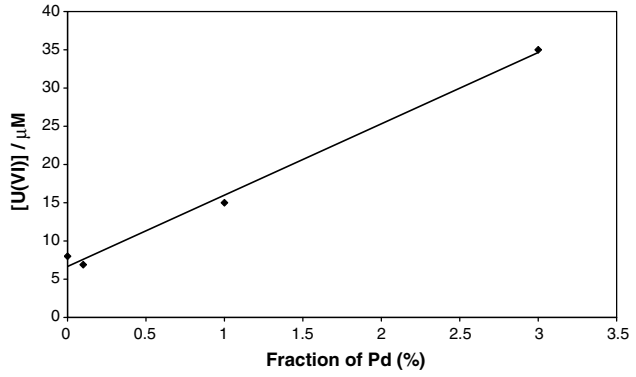

Fig. 1. Concentration of dissolved U(VI) after 50 min under N_2 atmosphere as a function of relative surface coverage of Pd.

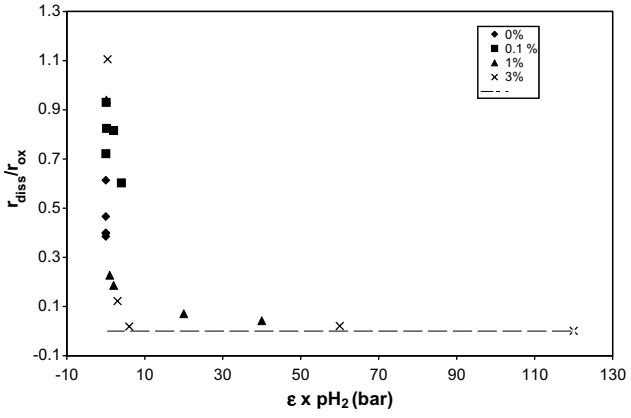

Fig. 2. Ratio between rate of uranium dissolution and rate of UO_2 oxidation (oxidant consumption) plotted against the relative surface area of Pd multiplied by the H_2 partial pressure (the dashed line represents $r_{diss} = 0$).

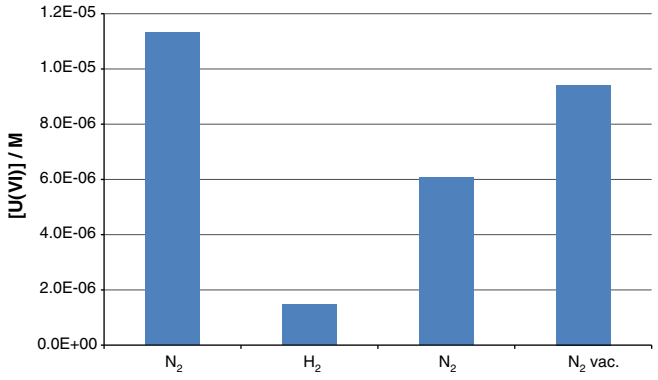

Fig. 3. Concentration of dissolved U(VI) after 50 min for four consecutive experiments under (1) N_2 atmosphere, (2) 40 bar H_2, (3) under N_2 atmosphere and (4) under N_2 atmosphere after vacuum treatment.

$$k_{H_2} = \frac{r_{ox}}{\varepsilon_{rel}[H_2]}. \quad (7)$$

From the data in Table 2, the solubility of H_2 and the total surface area of the pellet we obtain values of 4×10^{-7} m s^{-1} and 7×10^{-6} m s^{-1} for the pellets containing 1% and 3% Pd, respectively. The diffusion controlled rate constant for this system is expected to be in the order of 10^{-6} m s^{-1} [13]. Hence, the inhibiting reaction appears to be close to diffusion controlled. The slight difference in estimated rate constant between the two pellets may in fact have some relevance. In the pellet containing lower amount of Pd, every Pd particle must catalyze the solid phase or surface reduction for a larger UO_2 surface area than in the pellet containing higher amount of Pd. The electrical conductivity may then become a limiting factor causing the apparent difference in rate constant as proposed by Broczkowski et al. [23].

These results clearly demonstrate that the previously proposed mechanism for noble metal particle catalyzed H_2 inhibition of radiation induced dissolution of spent nuclear fuel appears to be correct and that the kinetics is virtually diffusion controlled. This is further evidenced by the use of this mechanism and the diffusion controlled rate constant when simulating (using the steady-state approach) the dynamics of a spent fuel dissolution experiment performed in a closed system taking radiolytic production of H_2 into account [18]. The dynamics of the system is very well reproduced by the simulation.

Acknowledgement

The Swedish Nuclear Fuel and Waste Management Company (SKB) is gratefully acknowledged for financial support.

References

[1] R.L. Segall, R.S.C. Smart, J. Nowotny, Surface and Near-Surface Chemistry of Oxide Materials, Elsevier Science Publishers B.V., Amsterdam, Netherlands, 1988. 527.
[2] D. Rai, A.R. Felmy, J.L. Ryan, Inorg. Chem. 29 (1990) 260.
[3] I. Casas, J. de Pablo, J. Giménez, M.E. Torrero, J. Bruno, E. Cera, R.J. Finch, R.C. Ewing, Geochim. Cosmochim. Acta 62 (1998) 2223.
[4] J.W.T. Spinks, R.J. Woods, An Introduction to Radiation Chemistry, John Wiley and Sons Inc., New York, 1964. 477.
[5] O. Roth, M. Jonsson, Cent. Eur. J. Chem. 6 (2008) 1.
[6] I. Grenthe, F. Diego, F. Salvatore, G. Riccio, J. Chem. Soc. Dalton Trans. 11 (1984) 2439.
[7] J. de Pablo, I. Casas, J. Gimenez, M. Molera, M. Rovira, L. Duro, J. Bruno, Geochim. Cosmochim. Acta 63 (1999) 3097.
[8] D.E. Grandstaff, Econ. Geol. 71 (1976) 1493.
[9] W.J. Gray, J.C. Tait, S.A. Steward, D.W. Shoesmith, High Level Radioactive Waste Management, in: V Annual International Conference, La Grange Park, IL, 1994, p. 2597.
[10] E.M. Pierce, J.P. Icenhower, R.J. Serne, J.G. Catalano, J. Nucl. Mater. 345 (2005) 206.
[11] D.W. Shoesmith, J. Nucl. Mater. 282 (1) (2000) 1.
[12] E. Ekeroth, M. Jonsson, J. Nucl. Mater. 322 (2003) 242.
[13] M.M. Hossain, E. Ekeroth, M. Jonsson, J. Nucl. Mater. 358 (2006) 202.
[14] E. Ekeroth, O. Roth, M. Jonsson, J. Nucl. Mater. 355 (2006) 38.
[15] F. Nielsen, K. Lundahl, M. Jonsson, J. Nucl. Mater. 372 (2008) 32.
[16] F. Nielsen, M. Jonsson, J. Nucl. Mater. 359 (1) (2006) 1.
[17] F. Nielsen, E. Ekeroth, T.E. Eriksen, M. Jonsson, J. Nucl. Mater. 374 (2008) 286.
[18] T.E. Eriksen, M. Jonsson, J. Merino, J. Nucl. Mater. 375 (2008) 331.
[19] M. Jonsson, F. Nielsen, O. Roth, E. Ekeroth, S. Nilsson, M.M. Hossain, Environ. Sci. Technol. 41 (2007) 7087.
[20] T.E. Eriksen, M. Jonsson, SKB Technical Report TR-07-06, 2007, p. 1.
[21] P. Carbol, J. Cobos-Sabathe, J.-P. Glatz, C. Ronchi, V. Rondinella, D.H. Wegen, T. Wiss, A. Loida, V. Metz, B. Kienzler, K. Spahiu, B. Grambow, J. Quiñones, A.M.E. Valiente, SKB Technical Report TR-05-09, 2005, p. 1.
[22] E. Cera, J. Bruno, L. Duro, T.E. Eriksen, SKB Technical Report TR-06-07, 2006, p. 1.
[23] M.E. Broczkowski, J.J. Noël, D.W. Shoesmith, J. Nucl. Mater. 346 (2005) 16.
[24] S. Nilsson, M. Jonsson, J. Nucl. Mater. 372 (2008) 160.
[25] S. Nilsson, M. Jonsson, J. Nucl. Mater. 374 (2008) 290.
[26] S.B. Savvin, Talanta 8 (1961) 673.
[27] I.K. Kressin, Anal. Chem. 56 (1984) 2269.